Ann. Phys. (Leipzig) **16**, No. 10–11, 767 – 779 (2007) / **DOI** 10.1002/andp.200710261

Circuit-QED: How strong can the coupling between a Josephson junction atom and a transmission line resonator be?

Michel Devoret[1,2,*], **Steven Girvin**[1], and **Robert Schoelkopf**[1]

[1] Applied Physics Department, Yale University, New Haven, CT 06520-8284, USA
[2] Collège de France, 75231 Paris cedex 05, France

Received 11 August 2007, accepted 14 August 2007
Published online 10 October 2007

Key words Superconductivity, Josephson effect, mesoscopic physics
PACS 03.67.Lx, 73.23.Hk, 32.80.-t

This article is dedicated to Hermann Grabert on the occasion of his 60th birthday.

After reviewing the limitation by the fine structure constant α of the dimensionless coupling constant of an hydrogenic atom with a mode of the electromagnetic field in a cavity, we show that the situation presents itself differently for an artificial Josephson atom coupled to a transmission line resonator. Whereas the coupling constant for the case where such an atom is placed inside the dielectric of the resonator is proportional to $\alpha^{1/2}$, the coupling of the Josephson atom when it is placed in series with the conducting elements of the resonator is proportional to $\alpha^{-1/2}$ and can reach values greater than 1.

1 Introduction

The field of quantum-mechanical Josephson junction circuits, of which Hermann Grabert has been one of the pioneers, does not have yet a universally adopted name: if we refer to Tony Leggett's original proposal of testing the validity of Quantum Mechanics at the macroscopic scale using these systems, we might call it Macroscopic Quantum Mechanics. Others might call this domain Mesoscopic Superconductivity to stress its relationship with the group of mesoscopic transport phenomena involving devices containing many atoms but only few quanta of excitations above the ground state. Recently, experiments performed at Yale on versions of such circuits incorporating microwave transmission lines have been described using the term Circuit Quantum Electrodynamics (circuit-QED), which refer to close similarities with the field of Cavity Quantum Electrodynamics (cavity-QED) belonging to Quantum Optics. One of us (M.D.) has also lately been using the term Quantum Radio-Electricity as a tongue-in-cheek reminder that we are often simply retracing the steps already taken many decades ago by radio engineers, but with circuit elements that now obey, at the level of collective variables like voltages and currents, quantum mechanics instead of classical laws. Sometimes, quantum mechanics just puts a slight twist on the usual behavior of the circuit. However, in certain circumstances, new effects which have no classical counterpart arise. Arriving at a clear understanding of these specific features of quantum circuits by using the minimum quantum formalism is the challenge of this domain. Also, the large flexibility of circuit designs offers new opportunities for experiments which in the future may help us understand better the core structure of Quantum Mechanics. By shedding light on very subtle quantum effects while at the same time always being willing to examine in detail the crude experimentalist models built with simple circuit elements, Hermann Grabert has set an example going in this direction.

Unlike natural atoms, Josephson circuits behaving as artificial atoms can be coupled to the electromagnetic field with arbitrarily large strength. How does this occur? Answering this question is the purpose of

* Corresponding author E-mail: michel.devoret@yale.edu

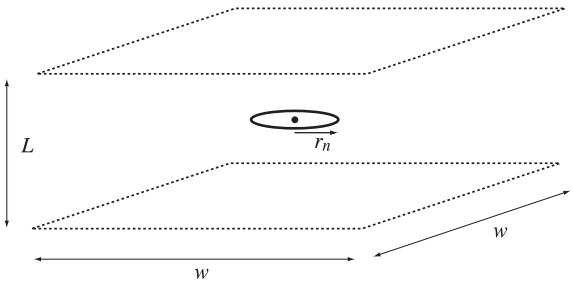

Fig. 1 Schematic view of a Rydberg atom placed inside a Fabry-Perot cavity. The mirrors are parallel and square for simplicity. A circular Rydberg state is considered. The radius of the semi-classical electron orbit is denoted r_n.

these notes. For their compatibility with recently published literature and in recognition of the scientific culture of Hermann which largely encompasses quantum optics, we will follow most of the cavity- and circuit-QED notations.

2 Review of the magnitude of the coupling between an atom and the electromagnetic field

Let us for simplicity – and direct relevance to most quantum optics experiments – consider an hydrogenic atom such as Rubidium or Cesium. We also make the additional hypothesis that the atom is excited in a circular Rydberg state: $n = l+1 = |m|+1 \gg 1$, where n, l and m are the usual principal (or radial), orbital and magnetic quantum number of atomic physics, respectively. This hypothesis does not actually restrict much the generality of our argument, but reduces all calculations to the bare minimum. The arguments developed in this section follow almost verbatim those found in the book by Haroche and Raimond [1], a basic graduate text on quantum physics, which also describes in detail the beautiful experiments performed on these circular Rydberg atoms. The arguments can be transposed qualitatively to the more usual states of atomic physics by taking the limit $n \to 1$.

For such electronic Rydberg states, we can adopt a semi-classical point of view and define an electron angular velocity ω_n around the circular orbit of radius r_n (the actual shape of the wavefunction is a doughnut, see Fig. 1). Quantum mechanics "à la Bohr" imposes a first relationship between these two quantities and we can write

$$m_e \omega_n r_n = p_n = \hbar k_n = \hbar \frac{n}{r_n} \,. \tag{1}$$

We thus get

$$\omega_n = \frac{\hbar n}{m_e r_n^2} \,. \tag{2}$$

Here m_e is the electron mass (we assume that the mass of the core is infinite). Another equation is obtained by following the usual treatment of the Kepler problem, i.e. by equating the centrifugal force and the centripetal force to which the electron is submitted:

$$m_e \omega_n^2 r_n = \frac{e^2}{4\pi\varepsilon_0 r_n^2} \,. \tag{3}$$

This yields

$$\frac{\hbar^2 n^2}{m_e r_n^3} = \frac{e^2}{4\pi\varepsilon_0 r_n^2} \,. \tag{4}$$

More rigorously, when we fix $l = n-1$ and $m = l$, we have a reduced Hamiltonian for the operator $\hat{\rho}$ corresponding to the radial distance between the nucleus and the electron. This reduced Hamiltonian reads

$$H_{\text{red}} = \frac{\hat{p}_\rho^2}{2m_e} + \frac{n\,(n-1)\,\hbar^2}{2m_e \hat{\rho}^2} - \frac{e^2}{4\pi\varepsilon_0^2 \hat{\rho}} \,. \tag{5}$$

Minimizing this Hamiltonian with respect to $\hat{\rho}$ treated as a classical number and taking $n(n-1) \simeq n^2$ we go back to Eq. (4). The full quantum treatment shows that the width of the doughnut scales like $n^{1/2}$. Finally, we get:

$$r_n = a_0 n^2 \tag{6}$$

where the Bohr radius is

$$a_0 = \frac{4\pi\varepsilon_0 \hbar^2}{m_e e^2} \,. \tag{7}$$

Likewise, we obtain the energy of the state

$$E_n = \frac{1}{2} m_e \omega_n^2 r_n^2 - \frac{e^2}{4\pi\varepsilon_0 r_n} = -\frac{\mathrm{Ry}}{n^2} \tag{8}$$

where the Rydberg characteristic energy is given by

$$\mathrm{Ry} = \frac{m_e e^4}{8\varepsilon_0^2 h^2} \,. \tag{9}$$

In order to make the two microscopic constants of atomic physics, the Bohr radius and the Rydberg more meaningful, we use

$$\frac{1}{\varepsilon_0} = Z_{\mathrm{vac}} c \tag{10}$$

where $Z_{\mathrm{vac}} \simeq 377\,\Omega$ and c are the impedance of the vacuum and speed of light, and we introduce the fine structure constant

$$\alpha = \frac{Z_{\mathrm{vac}}}{2R_K} \simeq \frac{1}{137} \tag{11}$$

where R_K is the impedance quantum of mesoscopic physics

$$R_K = \frac{h}{e^2} \simeq 25.8\,\mathrm{k}\Omega \,. \tag{12}$$

With these constants, we can rewrite the Bohr radius and the Rydberg energy as

$$\begin{aligned} \mathrm{Ry} &= \frac{\alpha^2}{2} m_e c^2 \\ a_0 &= \frac{1}{\alpha} \frac{\hbar}{m_e c} \,. \end{aligned} \tag{13}$$

If we now compute the transition frequency $|E_n - E_{n\pm1}|/\hbar$ from $\partial E_n/\partial n$, we naturally come back to the angular velocity of the electron on its semi-classical orbit, as expected:

$$\omega_n = 2\frac{\mathrm{Ry}}{\hbar n^3} \,. \tag{14}$$

Note the Kepler scaling between the radius and period of the orbit in which $\hbar$ disappears, as we could have anticipated from above

$$\begin{aligned} r_n &= a_0 \left(\frac{2\mathrm{Ry}}{\hbar}\right)^{2/3} \frac{1}{\omega_n^{2/3}} \\ &= \left(\frac{e^2}{4\pi\varepsilon_0 m_e}\right)^{1/3} \frac{1}{\omega_n^{2/3}} \,. \end{aligned} \tag{15}$$

We now turn to the electric dipole moment of the transition $n \to n \pm 1$ between circular states:

$$d_n = \frac{er_n}{\sqrt{2}} = \frac{ea_0 n^2}{\sqrt{2}} \tag{16}$$

which follows simply from the projection of the circular motion of the electron around its orbit.

If we now apply the classical Larmor formula

$$P_r = \frac{e^2 \ddot{x}^2}{6\pi\varepsilon_0 c^3} \tag{17}$$

for the power P_r of the radiation emitted from a dipole, which we take of the form $ex\,(t) = d_n \cos(\omega_n t)$, we can find the spontaneous emission rate

$$\begin{aligned} \Gamma_{n\to n-1} &= \frac{P_r}{\hbar\omega_n} \\ &= \frac{4}{3}\frac{\mathrm{Ry}}{\hbar}\alpha^3 n^{-5}\,. \end{aligned} \tag{18}$$

Remarkably, the same result can be found by a totally different path in which we apply Fermi's Golden Rule:

$$\begin{aligned} \Gamma_{n\to n-1} &= \frac{2\pi}{\hbar} \sum_{\text{1 photon states } p} \left|\langle \mathrm{vac}, n|\vec{\mathcal{E}}\cdot\vec{d}|p, n-1\rangle\right|^2 \delta\left(E_p - \hbar\omega_n\right) \\ &= \frac{d_n^2\omega_n^3}{3\pi\hbar\varepsilon_0 c^3}\,. \end{aligned} \tag{19}$$

In this last expression, $\vec{\mathcal{E}}$ is the electric field, $\vec{d} = e\vec{r}$ the dipole moment of the atom and $|p\rangle$ denotes a generic 1-photon propagating state with given energy E_p, polarisation and wave vector direction. If we now compute the quality factor of the transition corresponding to spontaneous emission, we find

$$\boxed{\frac{\omega_n}{\Gamma_{n\to n-1}} = Q_n = \frac{3n^2}{2\alpha^3}\,.} \tag{20}$$

The well-known conclusion we can draw from this formula in which the mass of the electron disappears is very general: the sharpness of atomic lines is directly linked to the fact that we live in a world where α is a small number.

Let us now go through a further step and calculate the coupling energy between the atom, which we treat as just a system with two levels $(n, n-1)$, and one specific mode of the electromagnetic field confined by a Fabry-Perot cavity in which the atom is now placed. In contrast with the case of the atom in free space in which the propagating photon modes form a continuum, in the case of the atom in a cavity, the electromagnetic modes are discrete standing waves. We take the mode frequency of interest to be very near the atomic transition frequency.

It will be sufficient, for the sake of our discussion, to consider a mode consisting of a plane wave bouncing back and forth between two parallel square mirrors with width w separated by a length L (see Fig. 1). We will ignore diffraction effects due to the mirror edges. Again, the result will lead to a conclusion whose validity extends beyond this particular case.

We remind the reader that the Hamiltonian of an hydrogenic atom in a time-varying electromagnetic field is given to an excellent approximation by

$$H = \frac{1}{2m_e}\left(\vec{p} + e\vec{\mathcal{A}}\right)^2 - \frac{e^2}{4\pi\varepsilon_0|\vec{r}\,|} \tag{21}$$

where $\vec{\mathcal{A}}$ is the vector potential of the time-varying part of the electromagnetic field in the Coulomb gauge ($\vec{\nabla} \cdot \vec{\mathcal{A}} = 0$). Relativistic, spin and core effects are absent from this 0-th order description.

The coupling Hamiltonian between atom and field is thus

$$H_c = \frac{e\vec{p} \cdot \vec{\mathcal{A}}}{m_e} \,. \tag{22}$$

This last relation can be canonically transformed into

$$H_c = e\vec{r} \cdot \vec{\mathcal{E}} \tag{23}$$

which is the basis of our Fermi Golden Rule expression written above.

We can compute the value of the matrix element of the electric field $\vec{\mathcal{E}}$ operator corresponding to a one-photon transition using the closure relation:

$$\sum_{N_{\rm ph}} \langle {\rm vac}|\vec{\mathcal{E}}\,|N_{\rm ph}\rangle\langle N_{\rm ph}|\vec{\mathcal{E}}\,|{\rm vac}\rangle = \langle {\rm vac}|\vec{\mathcal{E}}^2|{\rm vac}\rangle \,. \tag{24}$$

On the other hand, since photon modes are harmonic oscillators

$$\langle {\rm vac}|\vec{\mathcal{E}}\,|N_{\rm ph}\rangle = \begin{cases} \langle {\rm vac}|\vec{\mathcal{E}}\,|1\rangle & \text{when } N_{\rm ph} = 1 \\ 0 & \text{otherwise} \,. \end{cases} \tag{25}$$

Therefore

$$\begin{aligned} \left|\langle {\rm vac}|\vec{\mathcal{E}}\,|1\rangle\right| &= \left(\langle {\rm vac}|\vec{\mathcal{E}}^{\,2}|{\rm vac}\rangle\right)^{1/2} \\ &= \mathcal{E}^{\rm vac}_{\rm rms}. \end{aligned} \tag{26}$$

Here is a quick shortcut for computing the r.m.s. fluctuations of the electric field in the ground state (it works correctly for harmonic modes and should not hastily be generalized to non-linear ones). The instantaneous Poynting vector corresponding to a propagating plane wave is given by

$$|\vec{\mathcal{P}}(t)| = \frac{1}{Z_{\rm vac}} |\vec{\mathcal{E}}(t)|^2 \,. \tag{27}$$

Its average over one period is given by

$$\mathcal{P}_{\rm rms} = \frac{1}{Z_{\rm vac}} \mathcal{E}^2_{\rm rms} \,. \tag{28}$$

On the other hand, treating the vacuum state as a half-photon bouncing between two mirrors (this photon corresponds qualitatively to the zero-point energy), the energy flux in one direction can be computed semi-classically

$$\mathcal{P}^{\rm 1ph,1dir}_{\rm rms} = \frac{\hbar\omega_n}{4L/c} \frac{1}{w^2} \,. \tag{29}$$

Taking into account the standing wave character of the mode, we find

$$\mathcal{E}^{\rm vac}_{\rm rms} = \sqrt{\frac{cZ_{\rm vac}\hbar\omega_n}{Lw^2}} \,. \tag{30}$$

Introducing the mode volume

$$\mathcal{V} = Lw^2 \tag{31}$$

and its dimensionless version

$$\breve{\mathcal{V}} = \frac{Lw^2}{(\lambda/2)^3} \tag{32}$$

where

$$\lambda = \frac{2\pi c}{\omega_n} \tag{33}$$

we arrive at

$$\langle \mathrm{vac} \left| \mathcal{E} \right| 1 \rangle = \pi^{-3/2} \frac{\omega_n^2}{c} \sqrt{Z_{\mathrm{vac}} \hbar} \frac{1}{\sqrt{\breve{\mathcal{V}}}} \,. \tag{34}$$

The dimensionless coupling constant between the atom and the field mode, defined as the ratio of the vacuum Rabi frequency and the Larmor frequency,

$$\breve{g} = 2 \frac{d_n \langle \mathrm{vac} \left| \mathcal{E} \right| 1 \rangle}{\hbar \omega_n} \tag{35}$$

is thus proportional to $d_n \omega_n$ and given by

$$\breve{g} = \left(\frac{2}{\pi} \right)^{3/2} e \frac{a_0 \mathrm{Ry}}{\hbar^2 c n} \sqrt{Z_{\mathrm{vac}} \hbar} \frac{1}{\sqrt{\breve{\mathcal{V}}}} \,. \tag{36}$$

Using

$$a_0 \mathrm{Ry} = \alpha \hbar c \tag{37}$$

we arrive at our second important result

$$\boxed{\breve{g} \approx \frac{\alpha^{3/2}}{n} \frac{1}{\sqrt{\breve{\mathcal{V}}}} \,.} \tag{38}$$

We thus find that, due to the weakness of the fine structure constant, a discrete mode of a cavity is also always weakly coupled to the atom. In actual cavity-QED experiments, $\breve{g}$ is of order 10^{-6}.

However, a remarkable fact arises: the algebraic dependences of $\breve{g}$ and Q_n on n and α are such that when we compute one of the figures-of-merit of cavity-QED, namely the ratio of the coupling frequency to the decay rate of the excited level due to spontaneous emission, we find

$$\breve{g} Q_n \approx \alpha^{-3/2} n \frac{1}{\sqrt{\breve{\mathcal{V}}}} \,, \tag{39}$$

a number which, unlike $\breve{g}$ and $1/Q_n$, can be made much larger than 1 with appropriate experimental conditions. This last expression justifies the efforts by the various groups working in cavity-QED to go to small mode volumes and explains the focus on large principal numbers n by the Haroche group. Note that the number $\breve{g} Q_{\mathrm{cav}}$ describing the effect of photon losses in the cavity is the other important figure-of-merit which needs to be greater than unity for coherent vacuum Rabi oscillations between the cavity and the atom (strong coupling regime of cavity-QED).

We now turn to Josephson circuits, for which we will try to match, as closely as possible, the line of reasoning we have followed in this section to arrive at the relative strength of the atom-field coupling constants.

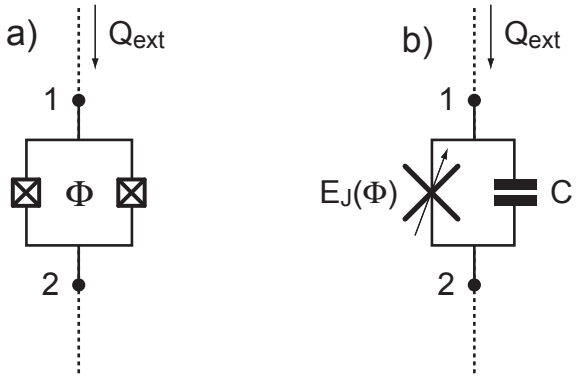

Fig. 2 (a) The split Cooper pair box consists of two junctions forming a loop and coupled to an external circuit providing a charge bias. No dc current is allowed to flow through the junctions, which behave as single adjustable Josephson element (cross) in parallel with a capacitance (b).

3 The Josephson junction atom

The tunnel junction circuit which is on par with the Rydberg atom is a circuit often referred to as the split Cooper pair box. It consists of two small Josephson junctions in parallel, forming a loop through which is threaded a constant flux Φ (see Fig. 2a). The inductance of the loop is very small compared to the effective inductance of the two junctions and they behave therefore as a single Josephson junction with adjustable Josephson energy $E_J(\Phi) = E_{J0}|\cos(\frac{e}{\hbar}\Phi)|$ (see Fig. 2b). The device is biased by an external circuit which only imposes time fluctuations of the charge having flown through the device, but no dc current.

The Hamiltonian of this split Cooper pair box can be written as

$$H = E_{\rm CP}\left(\hat{N} - \frac{\hat{Q}_{\rm ext}}{2e}\right)^2 - E_J(\Phi)\cos(\hat{\theta})\,. \tag{40}$$

The parameter $E_{\rm CP} = (2e)^2/2C_j$ is the charging energy in which C_j is the total capacitance of the two junctions. The phase operator $\hat{\theta}$ corresponds to the difference between the phase of the condensates of the superconducting electrodes separated by the junctions. It is conjugate to the number operator $\hat{N}$ corresponding to the total number of Cooper pairs having flown through the tunnel barrier between the two electrodes. Because $\hat{\theta}$ is an angle taking its values on a compact 1-d space, the commutation relation between $\hat{\theta}$ and $\hat{N}$ should be written as

$$\mathrm{e}^{i\hat{\theta}}\hat{N}\mathrm{e}^{-i\hat{\theta}} = \hat{N} - 1 \tag{41}$$

rather than the somewhat ill-defined relation

$$[\hat{\theta}, \hat{N}] = i\,. \tag{42}$$

The charge operator $\hat{Q}_{\rm ext}$ corresponds to the charge coupled by the external circuit into the device. Its role is similar to that of the vector potential $\vec{\mathcal{A}}$ in Eq. (21). It should be possible to draw an analogy between the reduced Hamiltonian of the circular Rydberg atom Eq. (5), supplemented with the correct electromagnetic term, and the Cooper pair box Hamiltonian Eq. (40). In this analogy, the role of the principal quantum number n of Rydberg atoms is played here by the ratio $E_J/E_{\rm CP}$. As we will see in more details below, the larger this ratio, the stronger the quantum fluctuations of the charge on the junction capacitance.

Let us examine how a particular biasing circuit modifies the Hamiltonian described by Eq. (40). Suppose we insert our Cooper pair box in a circuit consisting of a capacitance C in series with an inductance L (see Fig. 3). Applying the rules of quantum circuit theory [2], we find that the total Hamiltonian of the circuit reads

$$H_{\rm tot} = \frac{\hat{\Phi}^2_{\rm ext}}{2L} + \frac{\hat{Q}^2_{\rm ext}}{2C} + E_{\rm CP}\left(\hat{N} - \frac{\hat{Q}_{\rm ext}}{2e}\right)^2 - E_J\cos(\hat{\theta})\,. \tag{43}$$

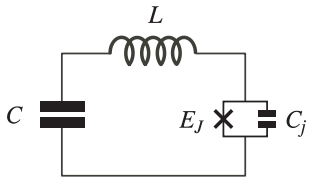

Fig. 3 Cooper pair box biased with a LC circuit. A flux through the inductance linearly varying in time can be used to impose a charge bias on the Cooper pair box.

The generalized flux and charge variables $\hat{\Phi}_{\rm ext}$ and $\hat{Q}_{\rm ext}$ are the operators corresponding to the time integral of the voltage across the external capacitor and the current flowing through the external inductor, respectively. They are canonically conjugate, obeying

$$[\hat{\Phi}_{\rm ext}, \hat{Q}_{\rm ext}] = i\hbar\,. \tag{44}$$

If we now suppose that the inductance L is so small that the energy $\hbar/\sqrt{LC}$ is bigger than any other energy in the problem, we can treat $\hat{N}$ and $\hat{\theta}$ as slow variables and $\hat{\Phi}_{\rm ext}$ and $\hat{Q}_{\rm ext}$ as fast variables. In the spirit of the Born-Oppenheimer approximation, we can replace $\hat{Q}_{\rm ext}$ by its average value $\tilde{Q}_{\rm ext}$ computed by treating $\hat{N}$ as a parameter. We find

$$\frac{\tilde{Q}_{\rm ext}}{C} - \frac{2e}{C_j}\left(\hat{N} - \frac{\tilde{Q}_{\rm ext}}{2e}\right) = 0\,. \tag{45}$$

Hence

$$\tilde{Q}_{\rm ext} = \frac{C}{C + C_j} 2e\hat{N}\,. \tag{46}$$

At the end of this calculation, we find that the Hamiltonian of the Cooper pair box is renormalized by the presence of the external circuit

$$H_{\rm ren} = E'_{\rm CP}\left(\hat{N} - N_g\right)^2 - E_J(\phi)\cos(\hat{\theta}) \tag{47}$$

where $E'_{\rm CP} = (2e)^2/2C_\Sigma$ is the usual charging energy including the total capacitance $C_\Sigma = C + C_j$. In this last formula, we have also included the constant charge offset $N_g = CU/2e$ produced by an additional voltage source U which would be in series with L and C. Note that it would have been easier to neglect from the start the inductance L, incorporate directly the external capacitance C in the capacitance of the junction since the two elements are now in parallel, and then write the quantum Hamiltonian of the modified circuit. This procedure works also for the more useful case when a series voltage source is inserted in the external circuit. We are witnessing here a commonly encountered circumstance in quantum circuits: ordinary circuit theory manipulations done before introducing non-commuting operators can often provide shortcuts to complex quantum mechanical calculations.

4 Energies and matrix elements of the Josephson atom

We will consider for simplicity the "transmon" case where $E_J \gg E_{\rm CP}$ which is also of interest for superconducting qubits [3], but our expressions can easily be generalized. For large $E_J/E_{\rm CP}$ the fluctuations in $\hat{\theta}$ are small and we can Taylor expand the cosine function to obtain

$$H \simeq E_{\rm CP}\left(\hat{N} - \frac{\hat{Q}_{\rm ext}}{2e}\right)^2 + E_J\frac{\hat{\theta}^2}{2} - E_J\frac{\hat{\theta}^4}{24}\,. \tag{48}$$

Introducing

$$b^\dagger = \frac{1}{\sqrt{2}}\left[\left(\frac{E_J}{2E_{\rm CP}}\right)^{\frac{1}{4}}\hat{\theta} + i\left(\frac{2E_{\rm CP}}{E_J}\right)^{\frac{1}{4}}\hat{N}\right]$$
$$b = \frac{1}{\sqrt{2}}\left[\left(\frac{E_J}{2E_{\rm CP}}\right)^{\frac{1}{4}}\hat{\theta} - i\left(\frac{2E_{\rm CP}}{E_J}\right)^{\frac{1}{4}}\hat{N}\right] \tag{49}$$

which obey

$$\left[b, b^\dagger\right] = 1 \tag{50}$$

we can write [3]

$$H \simeq \hbar\omega_{01} b^\dagger b - \left(\frac{2E_J}{E_{\rm CP}}\right)^{\frac{1}{4}}\left(\frac{b^\dagger - b}{i}\right)\frac{e\hat{Q}_{\rm ext}}{C_j} - \frac{E_{\rm CP}}{48}\left(b^\dagger + b\right)^4 \tag{51}$$

where

$$\hbar\omega_{01} = \sqrt{2E_{\rm CP}E_J}\,. \tag{52}$$

The states of the Josephson atom in the transmon regime are thus close to harmonic oscillator states. The relative anharmonicity is given by

$$\frac{\omega_{12} - \omega_{01}}{\omega_{01}} = -\sqrt{\frac{E_{\rm CP}}{32E_J}} + O\left[\left(\frac{E_{\rm CP}}{E_J}\right)^{3/2}\right]. \tag{53}$$

We can write the coupling between the Cooper pair box and the external circuit as

$$H_c = -2e\hat{N}\cdot\hat{V}_{\rm ext} \tag{54}$$

where the operator $\hat{V}_{\rm ext} = \hat{Q}_{\rm ext}/C_j$ represents the voltage developed by the external charge $\hat{Q}_{\rm ext}$ on the junction capacitance C_j. We see from this equation that $2e\hat{N}$ plays for the Cooper pair box the role of the dipole moment for the atom: the Josephson atom can be viewed crudely as a particle with charge 2e going back-and-forth between two capacitor plates across which the external circuit induces a voltage $\hat{V}_{\rm ext}$. The value of this analog of the dipole moment is

$$\left|\langle 0|2e\hat{N}|1\rangle\right| = \left(\frac{2E_J}{E_{\rm CP}}\right)^{\frac{1}{4}} e \tag{55}$$

This equation justifies why the ratio $E_J/E_{\rm CP}$ can be viewed as playing a role analogous to that of principal quantum number n.

5 Transmission line cavities

Unlike the Fabry-Perot cavities of quantum optics which are essentially three-dimensional, the transmission line cavities of circuit-QED are one-dimensional. As pointed out by two of us (S. G. and R. S.), the resulting determining advantage is a very reduced mode volume [4]. Here we will consider coplanar waveguide (CPW) transmission lines, which consist of a central wire running in the slot defined by two ground half-planes (Fig. 4a). They correspond to recent experiments performed on the quantum coherent coupling between

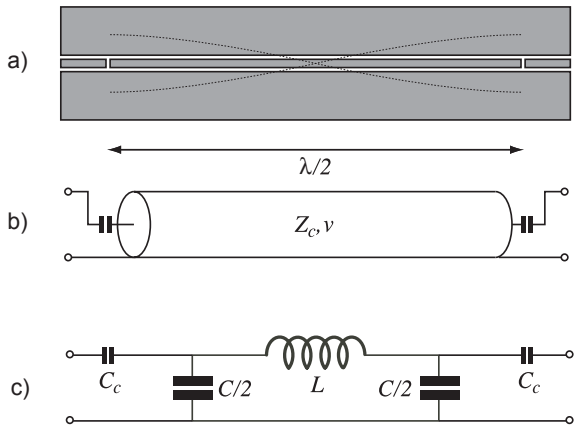

Fig. 4 (a) Coplanar waveguide transmission line resonator viewed from top. Grey areas are superconducting films. Dotted lines represent spatial variations of electric field between the center conductor and the ground planes for a $\lambda/2$ resonance. The system is a microwave analog of a Fabry-Perot resonator, the role of the mirrors being played here by the cuts in the center conductor. (b) Circuit schematic of transmission line resonator showing the "mirror" capacitances. The parameters Z_c and v are the impedance and propagation velocity of transmission line. (c) Discrete element model of resonator for frequencies in the vicinity of a $\lambda/2 = \pi v/\omega_0$ resonance.

superconducting qubits and cavities [5]. Other transmission lines such as microstriplines and coplanar microstriplines [6], can be used, but we will not deal with them here. Interrupting the central wire of the CPW by two in-plane capacitors makes a 1-d Fabry-Perot, the value of the capacitance determining the transmission coefficient of the "mirrors" .

It is convenient to model this distributed resonator with discrete elements. In general, if we deal with modes up to order m, we will need of order of m pairs of inductors and capacitors. Consider a $\lambda/2$ 1-d cavity resonating at frequency ω_0. The electric field between central and ground conductors is maximum at each end, while the current is maximal in the middle of the line (Fig. 4). We can model this cavity with one inductor L along its length and two capacitors $C/2$ at each end. The values of these elements should be taken such

$$\begin{aligned} \frac{1}{\sqrt{LC}} &= \omega_0 \\ \sqrt{\frac{L}{C}} &= Z_c \end{aligned} \tag{56}$$

where Z_c is the characteristic impedance of the CPW line, usually close to $50\,\Omega$. The "mirror" coupling capacitances C_c are such that

$$\frac{2C_c}{C} = Q_{\rm cav} \tag{57}$$

where $Q_{\rm cav}$ is the "loaded" quality factor of the cavity (we neglect the internal losses of the resonator, which in practice is made negligible with superconducting films).

Let us now compute the voltage V at the end of the resonator and the current I inside the resonator. For an electric harmonic oscillator, we have in the ground state

$$\langle 0|H|0\rangle = \frac{1}{2C}\langle 0|\hat{Q}^2|0\rangle + \frac{1}{2L}\langle 0|\hat{\Phi}^2|0\rangle = \frac{\hbar\omega_0}{2}\,. \tag{58}$$

Therefore, using the equipartition theorem,

$$\begin{aligned}\langle 0|\hat{Q}^2|0\rangle &= \frac{\hbar\omega_0 C}{2} = \frac{\hbar}{2}\frac{1}{Z_c}\\ \langle 0|\hat{\Phi}^2|0\rangle &= \frac{\hbar\omega_0 L}{2} = \frac{\hbar}{2}Z_c\,.\end{aligned} \tag{59}$$

We can transform these expressions and get

$$\begin{aligned}\langle 0|\hat{Q}|1\rangle &= e\sqrt{\frac{R_K}{4\pi Z_c}}\\ \langle 0|\hat{\Phi}|1\rangle &= \frac{h}{e}\sqrt{\frac{Z_c}{4\pi R_K}}\,.\end{aligned} \tag{60}$$

The voltage $\hat{V}$ is obtained from $\hat{\Phi}\omega_0$ and we get, accounting for the division over the two capacitors $C/2$

$$\begin{aligned}\langle 0|\hat{V}|1\rangle &= \frac{h\omega_0}{2e}\sqrt{\frac{Z_c}{4\pi R_K}}\\ &= \sqrt{\frac{1}{8\pi}}\frac{h\omega_0}{e}\sqrt{\frac{Z_c}{Z_{\rm vac}}}\alpha^{1/2}\,.\end{aligned} \tag{61}$$

The current $\hat{I}$ is obtained from $\hat{Q}\omega_0$ and we get

$$\begin{aligned}\langle 0|\hat{I}|1\rangle &= e\omega_0\sqrt{\frac{R_K}{4\pi Z_c}}\\ &= \sqrt{\frac{1}{8\pi}}e\omega_0\sqrt{\frac{Z_{\rm vac}}{Z_c}}\alpha^{-1/2}\,.\end{aligned} \tag{62}$$

6 Coupling schemes and associated dimensionless constants

We can couple the Josephson atom with the cavity in two different ways: a) we can place it in the gap between the central conductor and the ground plane, using the field maximum at each end of the resonator (equivalently we can use a λ cavity resonance and place our atom in the middle, as was done in the original circuit-QED experiment) or b) we can insert it in the central conductor of the cavity, half-way between the capacitors.

Coupling scheme (a) can be modeled by the circuit depicted in Fig. 5a where we introduce the capacitance C_g in series with the split Cooper pair box. We then find that

$$\langle 0|\hat{V}_{\rm ext}|1\rangle = \frac{C_g}{C_g + C_j}\langle 0|\hat{V}|1\rangle\,. \tag{63}$$

Combining this last equation with Eqs. (54), (55) and (61), the associated dimensionless coupling constant is thus

$$\breve{g}_\perp = \sqrt{\frac{1}{2\pi^3}}\left(\frac{2E_J}{E_{\rm CP}}\right)^{\frac{1}{4}}\sqrt{\frac{Z_c}{Z_{\rm vac}}}\frac{C_g}{C_g + C_j}\alpha^{1/2}. \tag{64}$$

We find here a situation similar to the coupling of an atom to a cavity mode: this dimensionless constant involves a positive power of the fine structure constant. Also, note that

$$\sqrt{\frac{Z_c}{Z_{\rm vac}}} < 1\,. \tag{65}$$

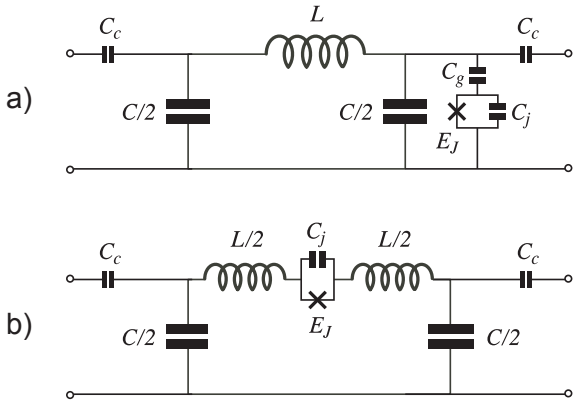

Fig. 5 Two different schemes for coupling a Josephson junction atom to a cavity resonator. (a) The junction is placed in the insulating gap of the transmission line and couples to its electric field. (b) The junction interrupts the central conductor of the resonator and is coupled to its current.

Nevertheless, because of the one-dimensional nature of the cavity α enters only through its square root rather than as $\alpha^{3/2}$ as in Eq. (38) and the condition $\breve{g}_\perp Q_{\rm cav}$ for strong coupling to the cavity can therefore be reached without going to extremely large $Q_{\rm cav}$. In practise, we have $\breve{g}_\perp \sim 10^{-2}$.

Coupling scheme (b) can be modeled by the circuit depicted on Fig. 5b. The Cooper pair box now directly couples to the $\hat{Q}$ operator of the resonator and thus $\hat{V}_{\rm ext} = \hat{Q}/C_j$. Using Eqs. (54), (55) and (62), the associated dimensionless constant is now given by

$$\begin{aligned}\breve{g}_\parallel &= 2\sqrt{\frac{1}{8\pi}}\left(\frac{2E_J}{E_{\rm CP}}\right)^{\frac{1}{4}}\sqrt{\frac{Z_{\rm vac}}{Z_c}}\alpha^{-1/2}\frac{e^2/C_j}{\sqrt{2E_{\rm CP}E_J}} \\ &= \sqrt{\frac{1}{8\pi}}\left(\frac{E_{\rm CP}}{2E_J}\right)^{\frac{1}{4}}\sqrt{\frac{Z_{\rm vac}}{Z_c}}\alpha^{-1/2}\,.\end{aligned} \tag{66}$$

We now find the even more favorable result that α enters with a negative power. Taking as an example the realistic values $Z_{\rm c} = 50\,\Omega$ and $E_{\rm CP}/2E_J = 100$, we arrive at the dimensionless coupling $\breve{g}_\parallel \simeq 20$. It is therefore possible to reach the ultra-strong coupling regime of cavity-QED [7]. The passage from coupling scheme (a) to coupling scheme (b) is a sort of duality transformation which interchanges the electric and magnetic field. In coupling scheme (a) the transmon couples to the electric field of the resonator like in usual cavity-QED experiment whereas in the "in-line" coupling scheme (b) the Josephson atom couples to the current, or in other words, to the magnetic field of the resonator. To our knowledge the consequences of this strong coupling have not yet been explored experimentally, although this junction-cavity in-line configuration has been used in the weak coupling regime for the Cavity Bifurcation Amplifier [8]. One immediate application of the strong coupling regime would be to make a simpler "in-line" transmon based on a CPW.

7 Conclusion

We have discussed comparatively the coupling to an electromagnetic cavity of a circular Rydberg atom, on one hand, and a Josephson junction atom, i.e. the Cooper pair box, on the other hand. It is possible with the latter to turn the smallness of the fine structure constant into an advantage when it comes to reaching ultra-strong coupling conditions. These conditions could be useful for making hybrid superconducting qubits which would store quantum information mostly into high-Q superconducting resonating cavities.

Acknowledgements Discussions with Vladmir Manucharian are gratefully acknowledged. This work was supported in part by the NSA under ARO contract number ARO W911NF-05-1-0365, and by the NSF under grants DMR-0653377 and DMR-0603369.

References

[1] S. Haroche and J.-M. Raimond, Exploring the Quantum: Atoms, Cavities and Photons (Oxford University Press, Oxford, 2006).

[2] B. Yurke and Denker, Phys. Rev. A **29**, 1419 (1984); M. H. Devoret, in: Quantum Fluctuations, edited by S. Reynaud, E. Giacobino, and J. Zinn-Justin (Elsevier, Amsterdam, 1997), p. 351; G. Burkard, R. H. Koch, and D. P. DiVincenzo, Phys. Rev. B **69**, 064503 (2004).

[3] J. Koch, T. M. Yu, J. Gambetta, A. A. Houck, D. I. Schuster, J. Majer, A. Blais, M. H. Devoret, S. M. Girvin, and R. J. Schoelkopf, to appear in Phys. Rev. A , arXiv:cond-mat/0703002. Note that the $E_{\rm CP}$ of the present article is 4 times larger than the single electron charging energy E_C used in this reference.

[4] A. Blais, R.-S. Huang, A. Wallraff, S. M. Girvin, and R. J. Schoelkopf, Phys. Rev. A **69**, 062320 (2004).

[5] A. Wallraff, D. I. Schuster, A. Blais, L. Frunzio, R.-S. Huang, J. Majer, S. Kumar, S. M. Girvin, and R. J. Schoelkopf, Nature **431**, 162 (2004); D. I. Schuster, A. A. Houck, J. A. Schreier, A. Wallraff, J. M. Gambetta, A. Blais, L. Frunzio, J. Majer, B. R. Johnson, M. H. Devoret, S. M. Girvin, and R. J. Schoelkopf, Nature **445**, 515 (2007).

[6] D. M. Pozar, Microwave Engineering (Wiley, Hoboken, 2005).

[7] C. Ciuti and I. Carusotto, Phys. Rev. A **74**, 033811 (2006).

[8] M. Metcalfe, E. Boaknin, V. Manucharyan, R. Vijay, I. Siddiqi, C. Rigetti, L. Frunzio, R. J. Schoelkopf, and M. H. Devoret, submitted to Phys. Rev. B, arXiv:0706.0765.